J. Biochem. **144,** 197–206 (2008)
doi:10.1093/jb/mvn059

Microglial Cell Death Induced by Glycated Bovine Serum Albumin: Nitric Oxide Involvement

Mohammad R. Khazaei[1,2], Mehran Habibi-Rezaei[1,*], Fereshteh Karimzadeh[2], Ali Akbar Moosavi-Movahedi[3], Abdo Alfattah Sarrafnejhad[4], Farzaneh Sabouni[5] and Mostafa Bakhti[1]

[1]School of Biology, College of Science, University of Tehran, Tehran, Iran; [2]International Graduate Research School of Molecular Basis of Dynamic Cellular Processes, Westfaelische Wilhelmes-Universitaet, Muenster, Germany; [3]Institute of Biochemistry and Biophysics; [4]Department of Health, Medical Sciences, University of Tehran; and [5]National Institute for Genetic Engineering and Biotechnology, Tehran, Iran

Received December 22, 2007; accepted April 15, 2008; published online May 7, 2008

Nonenzymatic glycation results in the formation of advanced glycation end products (AGEs) through a nonenzymatic multistep reaction of reducing sugars with proteins. AGEs have been suspected to be involved in the pathogenesis of several chronic clinical neurodegenerative complications including Alzheimer's disease, which is characterized with the activation of microglial cells in neuritic plaques. To find out the consequence of this activation on microglial cells, we treated the cultured microglial cells with different glycation levels of Bovine Serum Albumin (BSA) which were prepared *in vitro*. Extent of glycation of protein has been characterized during 16 weeks of incubation with glucose. Treatment of microglial cells with various levels of glycated albumin induced nitric oxide (NO) production and consequently cell death. We also tried to find out the mode of death in AGE-activated microglial cells. Altogether, our results suggest that AGE treatment causes microglia to undergo NO-mediated apoptotic and necrotic cell death in short term and long term, respectively. NO production is a consequence of iNOS expression in a JNK dependent RAGE signalling after activation of RAGE by AGE–BSA.

Key words: advanced glycation end products, apoptosis, glycation, microglia, nitric oxide.

The high level of blood sugar in diabetic patients (hyperglycemia) increases the rate of nonenzymatic glycation of proteins (*1*), which also occurs in normal individuals but at very lower rate (*2*). Nonenzymatic glycation is a process by which reducing sugars react with free amino groups in proteins through a series of reactions known as the Millard reaction. In this process, a Schiff base is formed between an amine group of a residue (*e.g.* Lys or Arg) in the protein and the carbonyl group of a reducing sugar. This step is followed by Amadori rearrangement to give dicarbonyl compounds or the early glycation products. The next step includes the formation of numerous intermediary products among which some are very reactive. Most recently the formation of molten globule-like state has been reported during progression of glycation reaction *in vitro* (*3*). The final step consists of crosslink formation between products in which heterogeneous structures called advanced glycation end products (AGE) are formed (*4*). There is increasing evidence that AGEs contribute to development of Alzheimer's disease (AD) and some other neuropathies in diabetics (*5–8*). Accordingly, many studies have demonstrated that the incidence and severity of AD are increased in individuals subjected with diabetes (*8*, *9*). AGE-proteins are recognized by receptor of AGE (RAGE) on microglial cells and this binding induces microglial activation via RAGE-signalling pathway (*10*). AGE-proteins can cause apoptotic cell death in some cell types (*11*, *12*), and they may also induce microglial apoptosis (*13*, *14*). Microglial apoptosis, has been implicated in several inflammatory disorders of the central nervous system (CNS) including AD (*15*, *16*), and multiple sclerosis (MS) (*17*). The relationship between AGE-protein induced activation and apoptosis of microglial cells, however, has not yet been clearly elucidated.

In this study, we propose that treatment of AGE-proteins on microglial cells induces microglial cell death in a RAGE -involved process. Microglial cells were treated with different glycation levels of Bovine Serum Albumin (BSA) (early glycated BSA to advance glycated BSA) which were prepared *in vitro*. A significant correlation between extent of glycation and the level of activation of microglial cells was observed. Furthermore, here we report that the levels of nitric oxide (NO) production correlates with cell death in accordance with the level of glycation. NO production is a consequence of iNOS expression in a JNK dependent RAGE signalling after activation of RAGE by AGE–BSA.

MATERIALS AND METHODS

Materials—Newborn rats (Wistar strain) were obtained from animal house of the university. The Dulbecco's Modified Eagle medium (DMEM) and fetal

*To whom correspondence should be addressed. Tel: +98-21-61113214, Fax: +98-21-66405141,
E-mail: mhabibi@khayam.ut.ac.ir

calf serum (FCS) from Gibco Life Technology, antibodies specific for the iNOS and tubulin from Abcam (Cambridge Science Park, UK), Specific JNK inhibitor SP600125 from Alexis Biochemical and $NaNO_2$ from Merck were purchased. Annexin V/propidium iodide (PI) staining Vybrant™ apoptosis assay kit was from Molecular Probes, Inc. Other chemicals used in this study were obtained from Sigma Chemical Company (St Louis, MO).

Cloning of sRAGE—The following primers were designed based on nucleotide sequence of human RAGE (Accession No. AB036432) and were used to clone sRAGE: forward (5′-TAA GAA TTC GCT CAA AAC ATC ACA GCC CG-3′) and reverse primers (5′-TAA CTC GAG TCA TTC GAT GCT GAT GCT GAC-3′). sRAGE was cloned between *Eco*RI and *Xho*I sites in pcDNA3.1vector containing Ig k-chain leader sequence as a secretory signal.

Preparation of Glycated BSA—Glycated BSA was prepared and characterized as described previously (*7*, *18*, *19*). In brief, BSA (0.75 mM) was reacted with D-glucose (50 mM) in 0.1 M phosphate buffer (pH 7.4) by incubation under sterile conditions at 37°C in the dark. To prevent bacterial contamination, 0.02% (w/v) NaN_3 was added to the solution and it was filtered through low protein binding filter (Millex.® -GV 0.22. μm filter unit, Millipore). After 0, 4, 8, 12 and 16 weeks, aliquots were taken from BSA–Glucose solution and were extensively dialyzed against autoclaved PBS at 4°C to remove unreacted glucose. The extent of glycation of BSA after each period of incubation was determined by measuring AGE associated fluorescence property as described elsewhere (*20*). Exciting at 370 nm, AGE-related autofluorescence of samples (0.15 mg/ml) was monitored in emission wavelength range of 400–500 nm. The spectra were corrected with appropriate protein and buffer blanks.

The amount of glycation was estimated using the 2,4,6-trinitrobenzenesulfonic acid (TNBS) assay (*21*). TNBS reacts specifically with free lysines and NH_2 terminal amino acid residues to form trinitrophenyl derivatives. The relative reduction of absorbance of glycated BSA compared with unmodified BSA is a linear function of the concentration of trinitrophenyl derivatives. Briefly 200 μl of samples (in which BSA concentration was 1 mg/ml) was mixed with 200 μl of 4% $NaHCO_3$, pH 8.4 and 200 μl of 5% TNBS in DMF. The mixture was incubated for 30 min at 52°C. Samples were cooled and optical density measured at 340 nm. The degree of glycation was calculated from the reduction of absorbance compared with unmodified BSA, and free amine content calculated using D-Glycine as a standard.

Isolation and Culture of Microglial Cells—Primary cultures of microglia from neocortex of newborn rats (Wistar strain) were prepared from mixed glial cultures according to the procedure of Giulian and Baker with some modifications (*22*). Briefly, meninges were removed and brain cortex tissue was minced in nutrient medium. Then cells were dissociated by triturating with fire-polished Pasteur pipettes to obtain a cell suspension. The cell suspension was plated at density of 5×10^4 cells/cm^2 into 25 cm^2 tissue culture flask (Nunc) in Dulbecco's Modified Eagle's Medium (DMEM), and 10% FCS at 37°C with 5% CO_2. Cells were fed every 4 days with a half change of the medium. After 2 weeks, cultures contained glial cells including rounded microglial cells mostly localized on the top of the astrocyte monolayer. The loosely adherent microglial cells were recovered by rigorously agitated for 30 min in an orbital shaker at 150 r.p.m. and 37°C (*23*). After centrifugation at 1,000 r.p.m. for 5 min, cells were cultured on 24 multiwell plates (Nunc) in DMEM supplemented with 10% FCS. After 15 min non-adherent cells were discarded and attached cells, mostly microglial, were harvested and plated at a final density of 1×10^6 cells/ml on 24 multiwell plates (Nunc) like previous step.

Cell Treatment—Before treatment, cells were subcultured on 24 multiwell plates at a density of 1×10^5 cells/ml in 10% FCS supplemented DMEM medium for 48 h, to enter the ramified phase in a semi-confluent culture. The culture medium replaced with medium in which composes of 10% BSA at different range of weeks (0, 4, 8, 12 and 16), instead of the 10% FCS. Also two experimental groups; with and without L-NG-monomethyl-L-arginine (L-NMMA) were prepared. Then treated cells incubated for 6, 12, 24 h and MTT assay method was performed to evaluate the viability of cells (*24*). In brief, the medium was replaced with 3-[4,5-dimethylthiazole-2-yl]-2,5-phenyltetrazolium bromide (MTT, 0.5 mg/ml) and incubated at 37°C for 4 h. After centrifugation at 1,000*g*, 100 μl supernatant were carefully removed and 100 μl DMSO was added to solubilize formazan crystals. The absorbance was measured at 540 nm using an EIA Multiscan MS microplate reader. At the same time, the microglial cells without treatment were analysed as control. To ensure the reproducibility of the results each assay was repeated three times.

Assessment of NO Synthesis—The production of NO by microglia was assessed through measuring nitrite in the supernatant of cultured cells. In brief, 100 μl of supernatant from each treatment was transferred to a 96-well flat-bottom microtiter plate and well mixed with equal volume of Griess reagent composed of 50 μl of sulfanilamide solution (1%) and 50 μl of 0.1% *N*-(1-Naphtyl)-ethylen-diamindihydrochloride (NEDA) solution, both in 2% phosphoric acid at room temperature for 10 min. The absorbance values at 550 nm were measured on an EIA Multiscan MS microplate reader. Fresh culture medium served as blank and $NaNO_2$ in a concentration range from 0 to 50 mM was used to construct standard curve (*25*). To assess the effect of NO production on microglial cells, they were treated with glycated BSA samples in the absence or presence of 200 μg/μl L-NMMA.

Characterization of the Mode of Death for Treated Microglia—The patterns of apoptosis and necrosis after cell treatment were assessed using acridine orange-ethidium bromide differential staining. A cell suspension of microglial cells (100 μl) which were under treatment for 6, 12 and 24 h, mixed with 10 μl of acridine orange (1 mg/l)-ethidium bromide (250 mg/l) solution and cells were analysed using a fluorescence microscope with 470 nm filter (Zeiss, Axioplan 2). For each sample, at least 200 cells were counted in different high-power

fields and the percentage of apoptotic and necrotic cells was calculated. While viable cells excluded ethidium bromide, acridine orange is intercalated into DNA, permitting assessment for nuclear chromatin condensation, margination and aggregation. Nuclei with chromatin aggregates were designated apoptotic. As cells were being counted, they were categorized into one of four groups: viable cell with uniform green fluorescent nuclei (V); Eerly apoptotic cells, which were viable but with condensed chromatin (EA); apoptotic cells, which were nonviable with an apoptotic nucleus (A); and necrotic cells, which were nonviable but contained a normal nucleus (N) (*26–28*). To ensure that significant under- or over-estimation of cell death was not occurring, the percentage of apoptotic and necrotic cells were determined by analyzing phosphatidylserine (PtdSer) externalization and membrane integrity by double staining with Annexin V and PI using flow cytometry as previously described (*29*, *30*) with a commercially available staining kit. Briefly, cells were harvested after the incubation and washed with cold PBS following with centrifugation at 900*g* for 10 min. The pellet was resuspended in annexin binding buffer to prepare a cell density of 1×10^6 cell/ml. Then 5 μl of Alexa Fluor 488 Annexin V and 1 μl of the 100 μg/ml PI solutions were added to 100 μl of cell suspension and incubated for 15 min. After incubation, 400 μl of annexin binding buffer was added and samples were kept on ice in dark. The treated cells were analysed by flow cytometry (Partec PAS-DAKO); measuring the fluorescence emission at 530 nm (*e.g.* FL1) and 600 nm (*e.g.* FL2). PI is impermeable to live cells and apoptotic cells, but stains necrotic cells with red fluorescence, binding tightly to the nucleic acids in the cell. After staining, apoptotic cells show green fluorescence, dead cells show red and green fluorescence and living cells show little or no fluorescence.

Treatment of Microglial Cells with sRAGE and JNK Inhibitor—To investigate the relation between AGE induced activation of microglial cells and production of NO, microglial cells were treated with AGE–BSA in the presence or absence of sRAGE. sRAGE is a soluble form of RAGE which acts as a decoy receptor and has been shown to prevent AGR–RAGE interaction and inhibit RAGE signalling (*31–33*). sRAGE was expressed in 293T HEK cells and administered to microglial cells in conditioned DMEM medium. For this reason, 293T HEK cells were transfected with sRAGE vector. Conditioned DMEM medium containing secreted sRAGE was collected after 3 days, and used for the microglial cell culture. The conditioned medium of 293T cells which had not been transfected, were used as a control. Microglial cells cultured in conditioned medium were treated with different glycation levels of BSA (AGE–BSA: 0, 4, 8, 12, 16) in the presence and absence of sRAGE for 24 h. Cell lysates were used for western blotting using anti-iNOS antibody (Abcam 1 : 1,000). To investigate if JNK is involved in RAGE signalling, AGE-induced microglia were treated with 20 μM SP600125, an inhibitor of JNK in dimethyl sulfoxide (DMSO), and after 24 h their lysates were used for western blotting. Comparable amount of protein were loaded for both of control and test samples, which has been documented using anti-tubulin antibody. The densities of ~130 kDa bands (for iNOS and tubulin, respectively) were determined using ImageJ software (released by NIH).

RESULTS

Preparation and Characterization of Glycated BSA—Autofluorescence is classically used to estimate the level of AGE formation (*19*). Fluorescence properties of the BSA molecules incubated with glucose were assessed to estimate AGE formation. Fluorescence studies over a 16-weeks incubation of BSA with glucose revealed an increase in the fluorescence intensity at 370/440 nm ($\lambda_{ex}/\lambda_{em}$). No increase in the intensity of autofluorescence was observed for control BSA solutions without glucose. Figure 1A shows fluorescence emission spectra in the range of 400–550 nm which have been presented in an ascending order of incubation time. The fluorescence intensity at maximum emission wavelength against weeks of incubation (inset to Fig. 1A) presents saturable nature and therefore site specificity of glycation of BSA. Succeeding spectra also show bathochromic effect along with the incubation weeks at almost 20 nm. These results reveal that our preparations contained a range of glycated BSA from low to high glycated BSA.

The amount of glycated amines was estimated by the TNBS assay. TNBS reacts specifically with free lysines. The relative reduction in absorbance of glycated BSA compared with unmodified BSA is a linear function of the concentration of trinitrophenyl derivatives. The free amine content decreased significantly from 8.84 to 4.6 mM after treatment with glucose during 16 weeks (Fig. 1B). Therefore, modification ratios of the lysine residues are deduced at 0% (corresponding to 8.84 mM free amine content), 20–30% (corresponding to 6–7 mM free amine content) and 40–50% (corresponding to 4–5 mM free amine content) for unmodified (control) BSA, early glycated BSA and advance glycated BSA, respectively.

Cell Viability—The total amount of cell death increased with the increment of the glycation level as assessed by MTT assay (Fig. 2). The viability of treated cells with AGE–BSA: 4 (BSA which is glycated for 4 weeks) was about 55% while cells treated with AGE–BSA: 16 (BSA which is glycated for 16 weeks) showed a massive cell death with cell viability reduced up to about 15%. The total amount of death for those cells treated in the presence of L-NMMA was significantly less than that induced to die by equivalent samples in the absence of L-NMMA. The inhibition of NO production in microglia was accompanied by a 2-fold increase in the number of viable cells. Cells treated with control; non-glycated BSA or AGE–BSA: 0, lived normally. For all treatments the cell viability decreased with longer treatment periods. To exclude the possible involvement of ROS generated from Amadori adducts microglial cells have also been treated with reduced glycated BSA. There were no significant differences in viability of treated cells with AGE–BSA: 16 and reduced-AGE–BSA: 16 (Supplementary Fig. S1).

Assessment of the NO Synthesis—Microglial cells were obtained as 95% pure culture and were treated with the

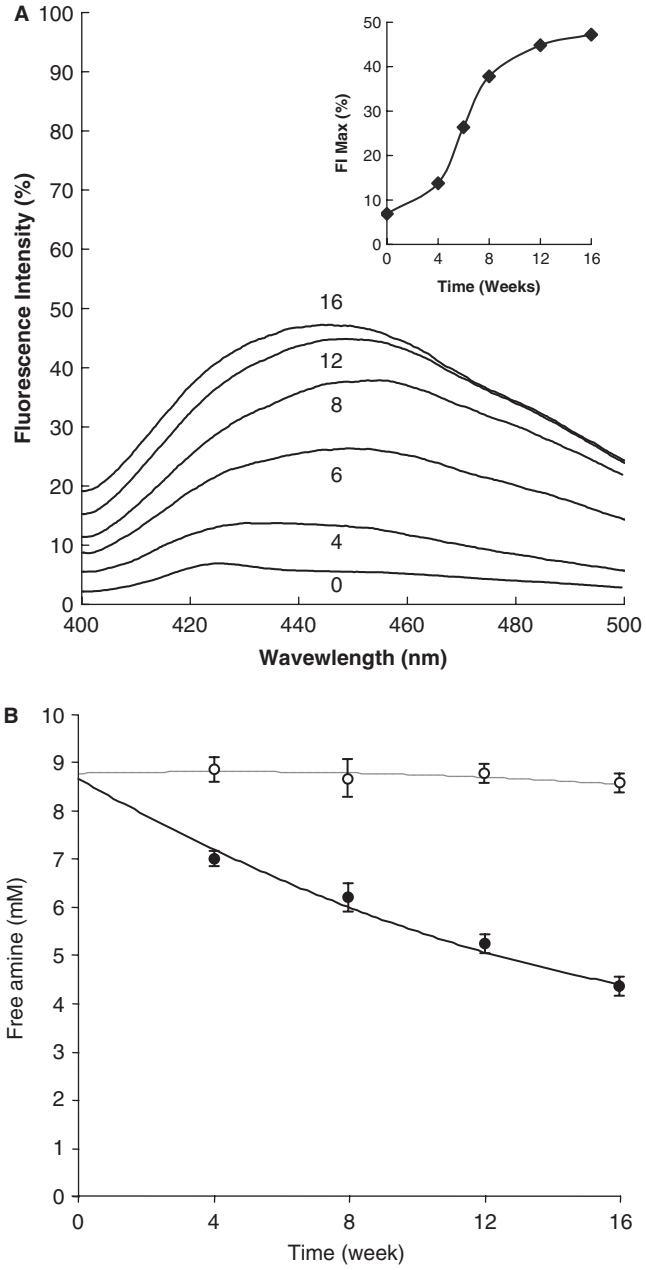

Fig. 1. **(A) Glycation time effect on AGE related fluorescence: spectrums were obtained in the wavelength range of 400–500 nm after excitation at 370 nm.** Protein concentration was used at 150 μg/ml. Inset to figure presents fluorescence intensity at maximum emission wavelength against weeks of incubation. During the same incubation time, autofluorescence intensity for control samples remained almost without change. Each spectrum belongs to a BSA solutions which was exposed for glycation for 0, 4, 6, 8, 12 and 16 weeks (AGE–BSA: 0, AGE–BSA: 4, etc.), respectively. (B) The amount of glycation was estimated using TNBS assay. The concentration of free amines (millimoles/liter) was calculated based on optical density of samples at 340 nm. The treadlines for the change in the concentration of free amines is shown. The dashed line and open circles indicate the control samples in the absence of glucose, and the continuous line and black circles indicate the free amines in samples incubated with glucose.

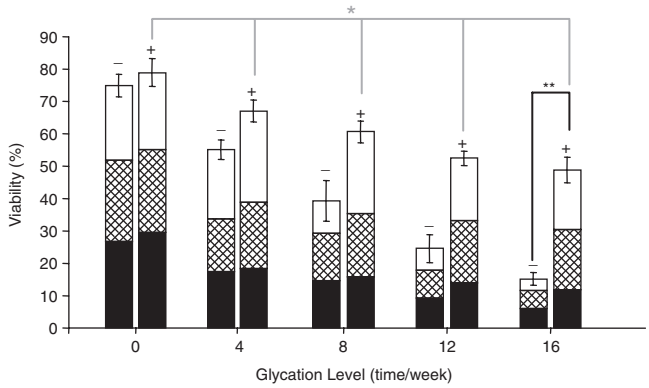

Fig. 2. **The effect of glycation level on cell viability; the effect of NOS inhibitor, L-NMMA has been presented.** Cells at 1×10^6/well in 24-well plates were treated with control or the indicated AGE–BSA for 6 h (open square), 12 h (cross hatched square) and 24 h (closed square), in the absence (−) or presence of L-NMMA (+). Percentage of cell viability was determined by MTT assay. [means ± SEM for three replications; $^{*}P \leq 0.01$ compared to treatment with unglycated BSA (week 0), $^{**}P \leq 0.01$ compared to treatments in the absence of L-NMMA].

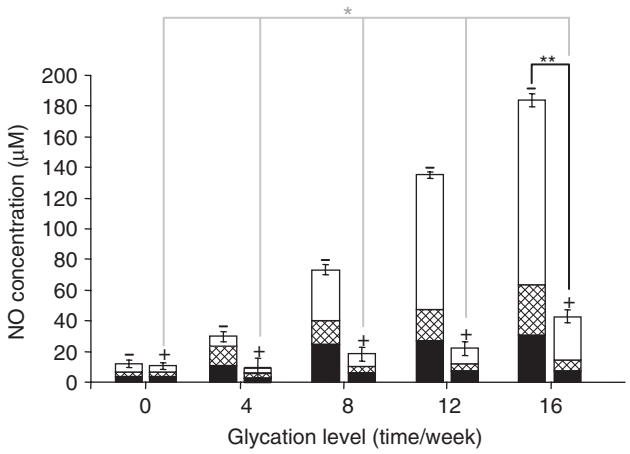

Fig. 3. **Effect glycation level of BSA on production of NO in microglial cell culture: cells at 1×10^6/well in 24-well plates were treated with AGE–BSA at different levels of glycation for 6 h (closed squares), 12 h (cross hatched square) and 24 h (open squares), in the absence (−) or presence of L-NMMA (+).** Culture media was removed and secreted NO was determined by measuring nitrite accumulation in the medium using Griess reagent. [means ± SEM for three replications; $^{*}P \leq 0.01$ compared to treatment with unglycated BSA (week 0), $^{**}P \leq 0.01$ compared to treatments in the absence of L-NMMA].

glycated BSA samples in the absence or presence of L-NMMA. Treated cells secreted NO, in response to treatment with glycated proteins. NO production increased as a function of glycation extent which was controlled through incubation time (in weeks). In addition, the concentration of secreted NO increased with lengthened cell treatment period (Fig. 3). In the absence of L-NMMA, glycated BSA samples in the range of AGE–BSA: 0 to AGE–BSA: 16, induced the production of substantial amounts of NO, but lower amounts of NO were produced from equivalent samples in the presence of L-NMMA. The inhibition of inducible NO synthase

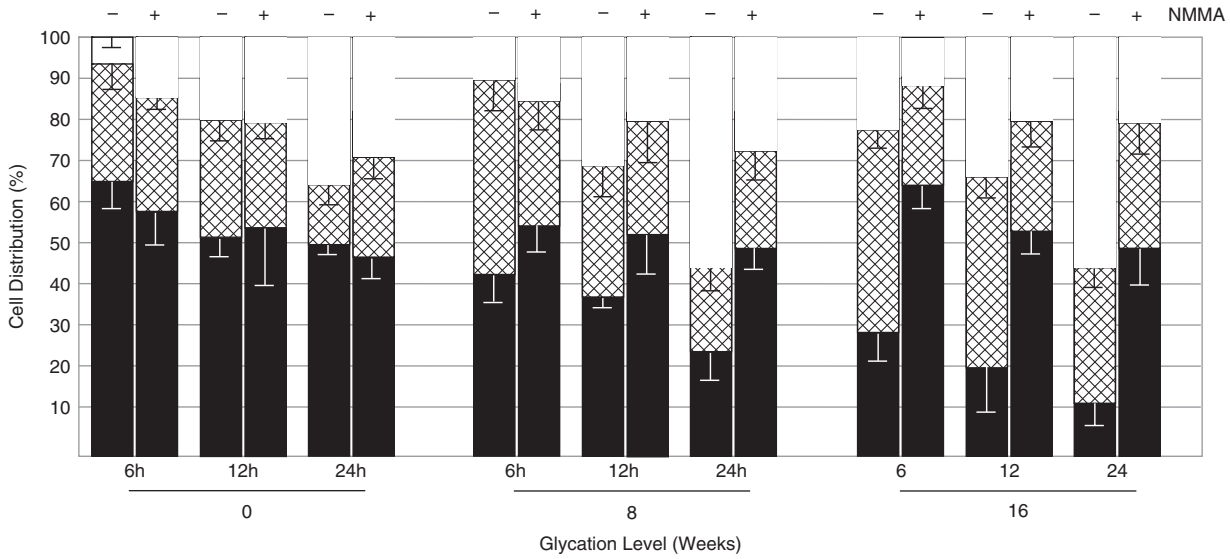

Fig. 4. **Distribution of viable (filled square), apoptotic (cross hatched square) and necrotic (open square) rat microglia treated with AGE–BSA: 16 for 6, 12 and 24 h in the absence (−) and presence (+) of L-NMMA was assessed using acridine orange-ethidium bromide differential staining method.** Cells were under treatment with appropriate AGE–BSA which were mixed with acridine orange-ethidium bromide solution and were analyzed using a fluorescence microscope with filter for 470 nm. (For details see MATERIAL AND METHODS).

(iNOS) by 200 μg/μl L-NMMA resulted in about 75% reduction in NO synthesis. The NO production in those cells treated with control (AGE–BSA: 0) was negligible. No significant differences in NO synthesis were observed between cells treated with AGE–BSA: 16 and reduced-AGE–BSA: 16 (Supplementary Fig. S2).

Acridine Orange-ethidium Bromide Differential Staining—Acridine orange is a cell-permeable dye that is being intercalated in DNA and results in a green colour appearance. Ethidium bromide enters cells with disrupted membrane integrity bind to RNA and double-stranded DNA to result in an orange appearance. Thus, differential uptake and binding of these dyes can determine early and late stages of apoptosis and necrosis (*28*, *34*). The photomicrographs of the acridine orange-ethidium bromide differential staining of the microglia after treatment with highly glycated BSA (AGE–BSA: 16) in the presence and absence of NOS inhibitor; L-NMMA for three different lengths of time (Supplementary Fig. S3) were analysed. The percentage of apoptotic, necrotic and viable cells after treatment with three levels of protein glycation; nonglycated- (AGE–BSA: 0), moderately-glycated- (AGE–BSA: 8) and highly-glycated-BSA (AGE–BSA: 16) for 6, 12 and 24 h are presented in Fig. 4. As expected, increase in percentage of apoptotic cells was observed with progression in inductive protein glycation. In agreement with NO production (Fig. 3), apoptosis induction was significantly lower for the cells which were not treated in comparison with treated cells. Experiments were performed three times and each point represents the mean of three assays. Reduction of AGE–BSA with 1 mM $NaCNBH_3$ did not have significant effect on the ability of AGE–BSA to induce apoptosis in microglial cells (Supplementary Figs S4 and S5).

Annexin V PI Staining—The PtdSer is normally localized in the inner leaflet but undergoes transbilayer movement during apoptosis and becomes exposed on the cell surface (*35*, *36*). Using Annexin V PI staining, it is possible to determine the index of cell apoptosis. Representative results of flowcytometry analysis for treatment of microglial cells with glycated BSA for 6 and 24 h are shown in Fig. 5. These data show that incubation of microglial cells with glycated BSA can decrease the viable population while the percentages of both apoptotic cells (PI −ve/Alexa +ve, lower right quadrant) and necrotic cells (PI +ve/Alexa +ve, upper right quadrant) were significantly increased by treatment with AGE–BSA samples. Furthermore, our complementary tests indicate that blocking NO production via administration of the arginine analog, L-NMMA, decreases the level of apoptosis in AGE–BSA treated samples (data are not shown). Prolonged treatment of the cells with the same level of glycated proteins from 6 to 24 h apparently resulted in decrease of the apoptotic cell percentage from 43.14 to 10.42 and concurrently increased necrotic cell percentage form 38.8 to 77.3. These observations show that microglial death quantified by Anexin V binding method correlates with the data from acridine orange/ethidium bromide labelling.

Effect of AGE–BSA on iNOS Expression—To investigate if raise in NO production after treatment with AGEs is due to change in the expression level of iNOS, the expression of iNOS in microglial cells after treatment with AGE–BSA was analysed by western blot. Microglial cells were treated with different glycation levels of BSA in the presence or absence of sRAGE. The expression level of iNOS in microglial cells was increased, by increase in the glycation level of BSA (Fig. 6A). However, no significant change was observed in the presence of sRAGE (Fig. 6B). This result indicates that increase in the level of iNOS and subsequently NO is mainly due to activation of RAGE signalling after treatment with AGEs.

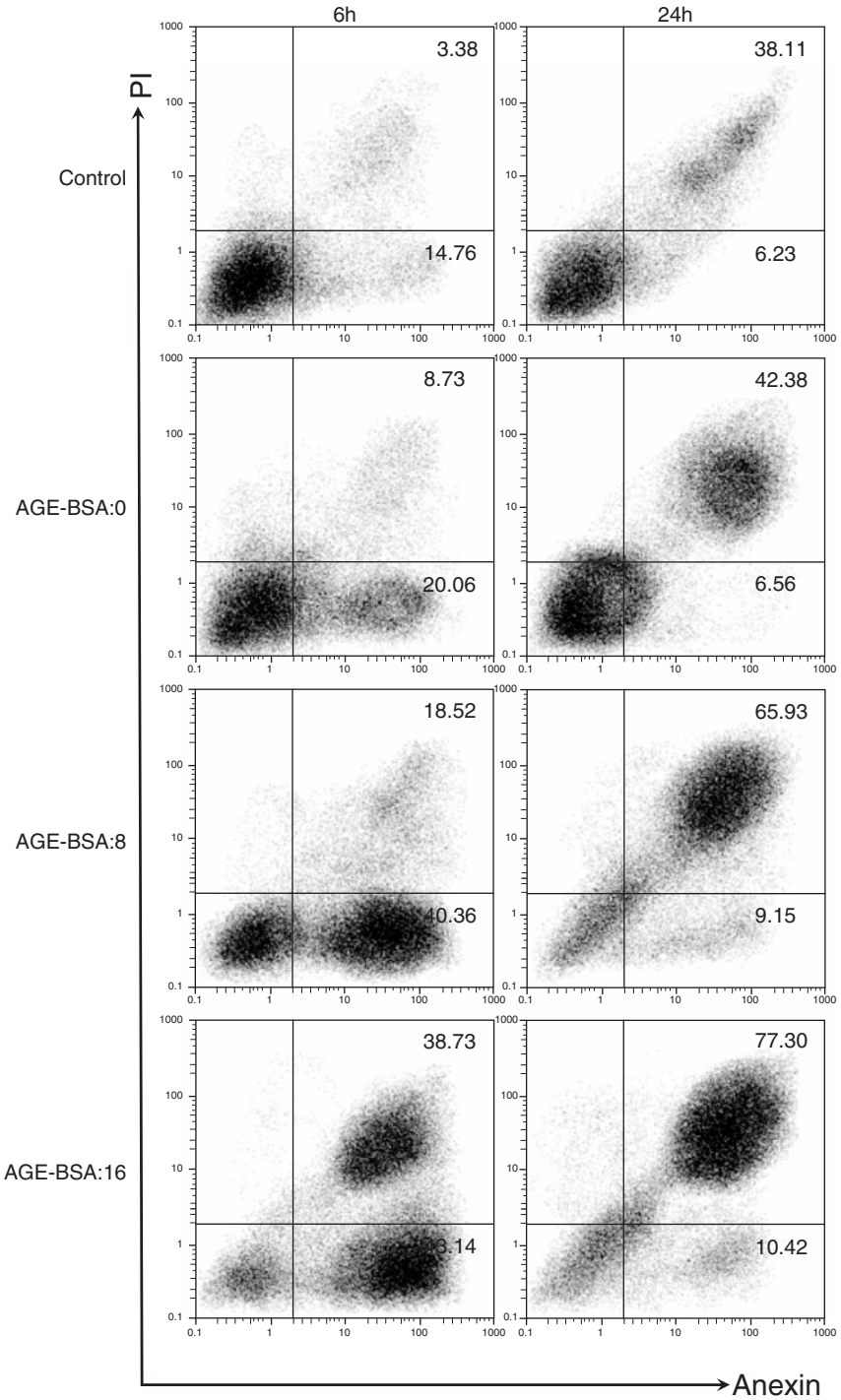

Fig. 5. **Dot-plots of PI versus Annexin V staining followed by flowcytometry analyses for microglia at density of 1×10^6 cell/ml, based on AGE-induced externalization of phosphatidylserin.** Controls are microglial cells without treatment; AGE–BSA: 0 represents microglial cells treated with non-glycated BSA for 6 or 24 h; AGE–BSA: 8 represents microglial cells treated with 8-weeks glycated BSA for 6 or 24 h and so on for others. The percentage of apoptotic and necrotic cells are presented and quantified in lower right and upper right quadrants, respectively.

JNK links AGE/RAGE to iNOS—It has been shown that Cdc42 and Rac1 are activated by RAGE which in turn results in activation of JNK (c-Jun NH_2-terminal kinase) signalling (*37–41*). JNK translocates to the nucleus where it can regulate the activity of multiple transcription factors which may involve in regulation of iNOS expression. To investigate if JNK can mediate AGE/RAGE signalling to iNOS expression, AGE-induced microglia were treated with JNK inhibitor, SP600125. Pharmacological inactivation of JNK resulted in

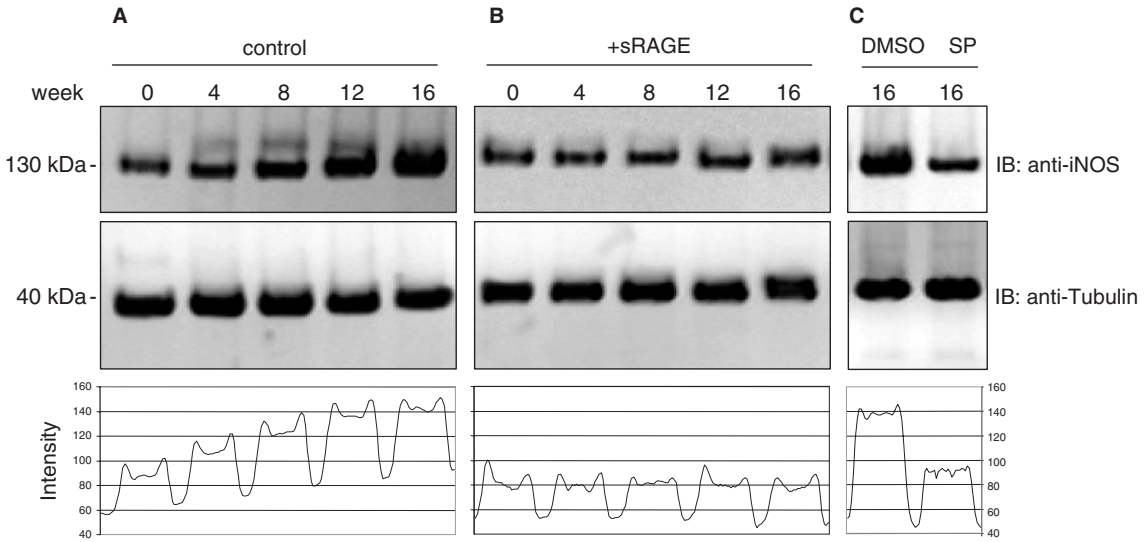

Fig. 6. **Western blot of iNOS protein expression in microglial cells.** Microglial cells were incubated with different glycated level of BSA in the absence (A) or the presence (B) of sRAGE for 24 h. To investigate if JNK is involved in pathway which link AGE/RAGE to iNOS expression, AGE-induced microglia were treated with DMSO (control) or 20 μM SP600125 (SP) (an inhibitor of JNK) (C). The expression of iNOS in microglial cell lysates was analysed by western blot using anti-iNOS antibody. An anti-tubulin antibody was used to confirm that comparable amounts of protein were loaded. The intensity of protein bands was determined by NIH ImageJ software, and has appended by the figure.

a reduction of iNOS level in AGE-stimulated microglia to those detected in their respective controls (Fig. 6C), suggesting that JNK activity is required for AGE/RAGE to up-regulate iNOS expression in microglia.

DISCUSSION

Under hyperglycemic conditions in diabetes, protein glycation and AGE formation increase. It has been shown that these AGE-proteins involve in development of many neuropathies, and patients with higher AGE-proteins are under higher risk of AD (*5–8*, *42*). However, it is unclear to date how the development of AD is related to glycated proteins. One of the primary cells which are damaged and lost in early stages of AD are microglial cells (*15*, *43–45*). It has been shown that in AD patient microglial cells first undergo an induction and activation process and then are eliminated by apoptosis (*15*, *16*). To find the link between glycated proteins and AD, we investigated the effect of glycated BSA on apoptosis of microglial cells. We treated microglial cells with different levels of *in vitro* prepared glycated BSA (from low to high glycated products; most probably corresponding with early to advance glycated products) at mild concentration of glycating sugar. These products were evaluated through their AGE-related autofluorescence and determination of free amine content (Fig. 1). A significant increase in activation and death of microglial cells was observed along with the increase in the glycation level of BSA (Fig. 2). This treatment also triggered the production of NO in microglia upon increasing the expression level of iNOS (Figs 3 and 6). It has been proposed that NO can cause apoptosis in microglial cells, probably due to oxidative stress and DNA damage and also release of cytochrome *c*, from the mitochondrial intermembrane space into the cytoplasm and consequently caspase activation (*46*). However, higher amounts of NO lead to necrotic cell death after making extreme cellular damage such as disrupting ion gradients, swelling the cell, rupturing the plasma membrane and NADH and ATP depletion (*46–49*). Therefore we investigated in parallel the effects of AGE–BSA on activation of microglial cells, NO secretion and the mode of cell death. When the viability and NO production were evaluated at different time points after AGE–BSA treatment, it was revealed that NO production is followed by cell death. A significant NO production was observed to be occurred after AGE–BSA treatment for exceeded incubation time from 12 h, while no significant decrease in cell viability was observed before this period. The release of NO accompanied by transformation of the microglial cells from rest to activated state and proceeded to cell death which occurred later. Highly glycated BSA induced more NO secretion (Fig. 3), and this was correlated with a significant increase in cell mortality. The observation that L-NMMA increases the viability of microglial cells (Fig. 2), suggests that a NO-mediated mechanism is involved in microglial cell death.

We next sought to determine whether the decrease in viability of microglial cells is due to apoptosis or other modes of cell death. The predominant mode of the microglial cell death after short-term treatment with AGEs was investigated to be apoptosis while in a long-term exposure, microglial cells start to undergo necrosis (Figs 4 and 5), most probably due to NO-inhibition of cytochrome *c* oxidase and NADH–Ubiquinone oxidorreductase in respiratory chain (*50*). However, evidence suggests that the two modes of cell death may not be as distinct as once thought and that apoptosis may, in some

systems, be followed by necrosis (*51*, *52*). The maximal PtdSer externalization was corroborated by morphological changes in nuclei at around 12 h after AGE administration which was followed by cell necrosis at around 24 h.

The percentage of microglial apoptosis increases with the increase in the glycation level and NO production. Furthermore, inhibition of iNOS by L-NMMA significantly blocked apoptosis of activated microglial cells, indicating that production of NO is responsible for apoptosis of the activated microglial cells. These results further support the role of NO in AGE-induced apoptosis of microglial cells. Several studies have been shown that NO induces apoptosis in microglia (*53*) and other cell types such as vascular smooth muscle cells (VSMCs) (*54*), macrophages (*55*), pancreatic islet (*56*), thymocytes (*57*) and neurons (*58*). Although it has been reported that low concentrations of NO exert an anti-apoptotic action in endothelial cells (*59–61*), hepatocytes (*62*) and trophoblasts (*63*), there are reports dealing with apoptotic effect of lower against higher amounts of NO on microglia (*64*). Therefore, it seems that the consequence of NO exposure on cells depends on cell type and the level of NO exposure.

Molecular mechanism which underlies the NO production after treatment with AGE–BSA is not fully understood yet. There is a report showing that Ras-MEK/ERK–NF-κB signalling pathway is involved in up-regulion of iNOS in microglial cells after activation of RAGE by AGE-Albumin. (*65*). However, we have indications that RAGE signalling via JNK pathway is involved in this process. We found that at concentrations which are likely to be attained in the brain extracellular compartment, AGEs up-regulates the expression of the iNOS in microglia (Fig. 6A) and the interaction of AGE–BSA with RAGE is necessary for up-regulation of iNOS and subsequently NO production (Fig. 6B). Moreover, results shown in Fig 6C indicate that induction of iNOS expression by AGE/RAGE in microglia, most probably is a JNK-dependent process. In the absence of JNK activity, the iNOS expression remains at the level comparable with non-induced (treated with AGE: 0) or competed binding (treated with sRAGE), even if microglial cells are highly stimulated with AGEs (Fig. 6C). The small GTPases, Cdc42 and Rac1, seem to play role in this pathway by activating JNK (*37*). JNK translocates to the nucleus where it can regulate the activity of multiple transcription factors which may involve in regulation of iNOS expression. Collectively, the data provided here put together with the results obtained by other groups (*37*, *41*, *64*) suggest that JNK activation by Cdc42/Rac1 is involved in up-regulation of iNOS in microglia through RAGE activation by AGE proteins (Fig. 7).

Altogether, our studies strongly suggest that AGE treatment causes microglia to undergo NO-mediated apoptosis in short-term exposure of cells and necrosis in longer exposure of cells to NO. The increase in NO production is a result of increase in expression level of iNOS, as a result of activation of JNK signalling. However, still it needs to investigate the pathologic mode of microglial cell death *in vivo* and diabetic patients' tissue.

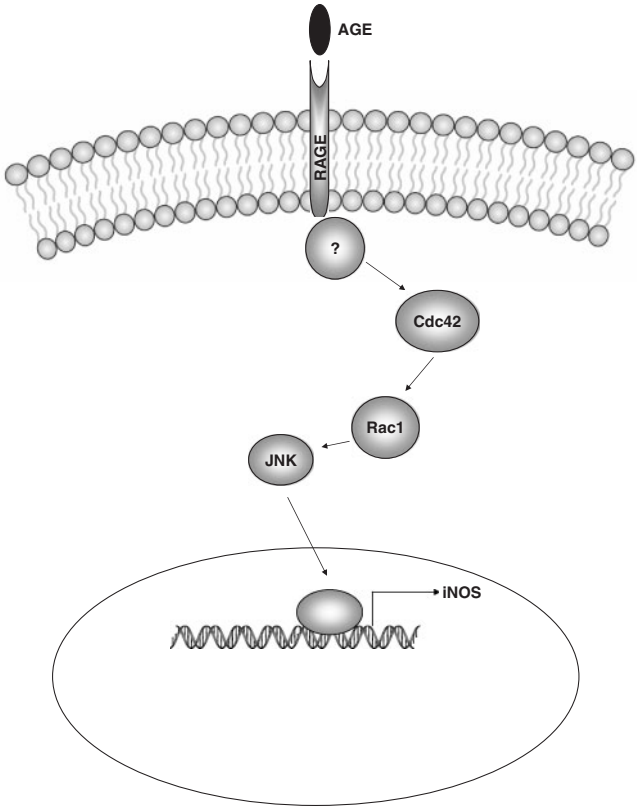

Fig. 7. **Schematic representation of the proposed mechanism of AGE/RAGE-dependent up-regulation of iNOS expression in microglial cells.** AGE-proteins bind to RAGE and activate it. The Cdc42/Rac1 pathway presented to be activated by AGE/RAGE which leads to JNK activation. Activated JNK translocates into the nucleus and activates transcription factors like Jun which stimulates iNOS expression.

Supplementary data are available at *JB* Online.

This research was supported in part by grants from Iran National Science Foundation (INSF) grant number 8308 and Research Council of University of Tehran. We thank Dr B. Shahsavan-Behboudi (School of Biology, University of Tehran) and Dr N. Müller (Department of Neurology, University of Münster) for their technical support and reagents, and S.A. Marashi (The IMPRS for Computational Biology and Scientific Computing, Berlin) for his fruitful comments on the manuscript.

REFERENCES

1. Monnier, V.M., Bautista, O., Kenny, D., Sell, D.R., Fogarty, J., Dahms, W., Cleary, P.A., Lachin, J., and Genuth, S. (1999) Skin collagen glycation, glycoxidation, and crosslinking are lower in subjects with long-term intensive versus conventional therapy of type 1 diabetes: relevance of glycated collagen products versus HbA1c as markers of diabetic complications. DCCT Skin Collagen Ancillary Study Group. Diabetes Control and Complications Trial. *Diabetes* **48**, 870–880
2. Monnier, V.M. and Cerami, A. (1981) Nonenzymatic browning in vivo: possible process for aging of long-lived proteins. *Science* **211**, 491–493
3. Sattarahmady, N., Moosavi-Movahedi, A.A., Ahmad, F., Hakimelahi, G.H., Habibi-Rezaei, M., Saboury, A.A., and Sheibani, N. (2007) Formation of the Molten Globule-Like

State during prolonged glycation of human serum albumin. *Biochim. Biophys. Acta* **1770**, 933–942
4. Monnier, V.M., Nagaraj, R.H., Portero-Otin, M., Glomb, M., Elgawish, A.H., Sell, D.R., and Friedlander, M.A. (1996) Structure of advanced Maillard reaction products and their pathological role. *Nephrol. Dial. Transplant* **11**, 20–26
5. Brownlee, M. (2000) Biochemistry and molecular cell biology of diabetic complications. *Nature* **414**, 813–820
6. Singh, R., Barden, A., Mori, T., and Beilin, L. (2001) Advanced glycation end products: a rewiev. *Diabetologia* **44**, 129–146
7. Valencia, J.V., Weldon, S.C., Quinn, D., Kiers, G.H., DeGroot, J., TeKoppele, J.M., and Hughes, T.E. (2004) Advanced glycation end product ligands for the receptor for advanced glycation end products: biochemical characterization and formation kinetics. *Anal. Biochem.* **324**, 68–78
8. Grossman, H. (2003) Does diabetes protect or provoke Alzheimer's disease? Insights into the pathobiology and future treatment of Alzheimer's disease. *CNS Spectr.* **8**, 815–823
9. Leibson, C.L., Rocca, W.A., Hanson, V.A., Cha, R., Kokmen, E., O'Brien, P.C., and Palumbo, P.J. (1997) Risk of dementia among persons with diabetes mellitus: a population-based cohort study. *Am. J. Epidemiol.* **145**, 301–308
10. Yan, S.D., Chen, X., Fu, J., Chen, M., Zhu, H., and Roher, A. (1996) RAGE and amyloid-β peptide neurotoxicity in Alzheimer's disease. *Nature* **382**, 685–691
11. Min, C., Kang, E., Yu, S.H., Shinn, S.H., and Kim, Y.S. (1999) Advanced glycation end products induce apoptosis and procoagulant activity in cultured human umbilical vein endothelial cells. *Diabetes Res. Clin. Pract.* **46**, 197–202
12. Yamagishi, S., Amano, S., Inagaki, Y., Okamoto, T., Koga, K., Sasaki, N., Yamamoto, H., Takeuchi, M., and Makita, Z. (2002) Advanced glycation end products-induced apoptosis and overexpression of vascular endothelial growth factor in bovine retinal pericytes. *Biochem. Biophys. Res. Commun.* **290**, 973–978
13. Dukic-Stefanovic, S., Gasic-Milenkovic, J., Deuther-Conrad, W., and Munch, G. (2003) Signal transduction pathways in mouse microglia N-11 cells activated by advanced glycation endproducts (AGEs). *J. Neurochem.* **87**, 44–55
14. Lee, P., Lee, J., and Kim, S. (2001) NO as an autocrine mediator in the apoptosis of activated microglial cells: correlation between activation and apoptosis of microglial cells. *Brain Research* **892**, 380–385
15. Streit, W.J., Sammons, N.W., Kuhns, A.J., and Sparks, D.L. (2004) Dystrophic microglia in the aging human brain. *Glia* **45**, 208–212
16. Yang, F., Sun, X., Beech, W., Teter, B., Wu, S., Sigel, J., Vinters, H.V., Frautschy, S.A., and Cole, G.M. (1998) Antibody to caspase cleaved actin detects apoptosis in differentiated neuroblastoma and plaque-associated neurons and microglia in Alzheimer's disease. *Am. J. Pathol.* **152**, 379–389
17. White, C.A., McCombe, P.A., and Pender, M.P. (1998) Microglia are more susceptible than macrophages to apoptosis in the central nervous system in experimental autoimmune encephalomyelitis through a mechanism not involving Fas (CD95). *Int. Immunol.* **10**, 935–941
18. Bourdon, E., Loreau, N., and Blache, D. (1999) Glucose and free radicals impair the antioxidant properties of serum albumin. *FASEB J.* **13**, 233–244
19. Westwood, M.E. and Thornalley, P.J. (1995) Molecular characteristics of methylglyoxal-modified bovine and human serum albumins. Comparison with glucose-derived advanced glycation endproduct-modified serum albumins. *J. Protein Chem.* **14**, 359–372
20. DeGroot, J., Verzijl, N., Wenting-van Wijk, M.J., Jacobs, K.M., Van El, B., Van Roermund, P.M., Bank, R.A., Bijlsma, J.W., TeKoppele, J.M., and Lafeber, F.P. (2004) Accumulation of advanced glycation end products as a molecular mechanism for aging as a risk factor in osteoarthritis. *Arthritis Rheum.* **50**, 1207–1215
21. Habeeb, A.F. (1966) Determination of free amino groups in proteins by trinitrobenzenesulfonic acid. *Anal. Biochem.* **14**, 328–336
22. Giulian, D. and Baker, T.J. (1986) Characterization of ameboid microglia isolated from developing mammalian brain. *J. Neurosci.* **6**, 2163–2178
23. Eugenín, E.A., Eckardt, D., Theis, M., Willecke, K., Bennett, M.V.L., and Sáez, J.C. (2001) Microglia at brain stab wounds express connexin 43 and in vitro form functional gap junctions after treatment with interferon-gamma and tumor necrosis factor-alpha. *Proc. Natl. Acad. Sci. USA* **98**, 4190–4195
24. Mosmann, T. (1983) Rapid colorimetric assay for cellular growth and survival: application to proliferation and cytotoxicity assays. *J. Immunol. Methods* **65**, 55–63
25. Fernandez-Botran, R. and Vetvicka, V. (2001) *Methods in cellular immunology* Boca Raton (USA), CRC Press
26. Duke, R.C. and Cohen, J.J. (1992) Morphological and biochemical assays of apoptosis in *Current Protocols in Immunology* (Coligan, J.E., Krvisbeek, A.M., Margulies, D.H., Shevach, E.M., & Strober, W, eds.) pp. 3.17.1–3.17.16, New York, Green Publishing and Wiley-Interscience
27. Kasibhatla, S., Amarante-Mendes, G.P., Finucane, D., Brunner, T., Bossy-Wetzel, E., and Green, D.R. (2006) Acridine orange/ethidium bromide (AO/EB) staining to detect apoptosis. *Cold Spring Harb Protoc.* doi:10.1101/pdb.prot4493
28. McGahon, A.J., Martin, S.J., Bissonnette, R.P., Mahboubi, A., Shi, Y., Mogil, R.J., Nishioka, W.K., and Green, D.R. (1995) The end of the (cell) line: methods for the study of apoptosis in vitro. *Methods Cell Biol.* **46**, 153–185
29. Fabisiak, J.P., Tyurina, Y.Y., Tyurin, V.A., Lazo, J.S., and Kagan, V.E. (1998) Random versus selective membrane phospholipid oxidation in apoptosis: role of phosphatidylserine. *Biochemistry* **37**, 13781–13790
30. van Engeland, M., Nieland, L.J.W., Ramaekers, F.C.S., and Schutte, B. (1998) Reutelingsperger CPM, annexin V-affinity assay: a review on an apoptosis detection system based on phosphatidylserine exposure. *Cytometry* **31**, 1–9
31. Deane, R., Du Yan, S., Submamaryan, R.K., LaRue, B., Jovanovic, S., and Hogg, E. (2003) RAGE mediates amyloid-beta peptide transport across the blood-brain barrier and accumulation in brain. *Nat. Med.* **9**, 907–913
32. Goova, M.T., Li, J., Kislinger, T., Qu, W., Lu, Y., Bucciarelli, L.G., Nowygard, S., Wolf, B.M., Caliste, X., Yan, S.F., Stern, D.M., and Schmidt, A.M. (2001) Blockade of receptor for advanced glycation end-products restores effective wound healing in diabetic mice. *Am. J. Pathol.* **159**, 513–525
33. Park, L., Raman, K., Lee, K., Lu, Y., Ferran, L., Chow, W.S., Stern, D., and Schmidt, A.M. (1998) Suppression of accelerated diabetic atherosclerosis by the soluble receptor for advanced glycation endproducts. *Nat. Med.* **4**, 1025–1031
34. Vento, R., Giuliano, M., Lauricella, M., Carabillo, M., Di Liberto, D., and Tesoriere, G. (1998) Induction of programmed cell death in human retinoblastoma Y79 cells by C2-ceramide. *Mol. Cell. Biochem.* **185**, 7–15
35. Homburg, C.H., de Haas, M., von dem Borne, A.E., Verhoeven, A.J., Reutelingsperger, C.P., and Roos, D. (1995) Human neutrophils lose their surface Fc gamma RIII and acquire Annexin V binding sites during apoptosis in vitro. *Blood* **15**, 532–540
36. Koopman, G., Reutelingsperger, C.P., Kuijten, G.A., Keehnen, R.M., Pals, S.T, and van Oers, M.H. (1994) Annexin V for flow cytometric detection of phosphatidylserine expression on B cells undergoing apoptosis. *Blood* **1**, 1415–1420

37. Bianchi, R., Adami, C., Giambanco, I., and Donato, R. (2007) S100B binding to RAGE in microglia stimulates COX-2 expression. *J. Leukoc. Biol.* **81**, 108–118
38. Coso, O.A., Chiariello, M., Yu, J.C., Teramoto, H., Crespo, P., Xu, N., Miki, T., and Gutkind, J.S. (1995) The small GTP-binding proteins Rac1 and Cdc42 regulate the activity of the JNK/SAPK signaling pathway. *Cell* **81**, 1137–1146
39. Huttunen, H.J., Fages, C., and Rauvala, H. (1999) Receptor for Advanced Glycation End Products (RAGE)-mediated neurite outgrowth and activation of NF-kappa B require the cytoplasmic domain of the receptor but different downstream signaling pathways. *J. Biol. Chem.* **274**, 19919–19924
40. Minden, A., Lin, A., Claret, F.X., Abo, A., and Karin, M. (1995) Selective activation of the JNK signaling cascade and c-Jun transcriptional activity by the small GTPases Rac and Cdc42Hs. *Cell* **81**, 1147–1157
41. Sorci, G., Riuzzi, F., Arcuri, C., Giambanco, I., and Donato, R. (2004) Amphoterin stimulates myogenesis and counteracts the antimyogenic factors basic fibroblast growth factor and S100B via RAGE Binding. *Mol. Cell. Biol.* **24**, 4880–4894
42. Takeda, A., Yasuda, T., Miyata, T., Goto, Y., Wakai, M., Watanabe, M., Yasuda, Y., Horie, K., Inagaki, T., Doyu, M., Maeda, K., and Sobue, G. (1998) Advanced glycation end products, co localized with asterocytes and microglial cells in Alzheimer's disease brain. *Acta Neuropathol.* **95**, 555–558
43. Dickson, D.W., Sinicropi, S., Yen, S.H., Ko, L.W., Mattiace, L.A., Bucala, R., and Vlassara, H. (1996) Glycation and microglial reaction in lesions of Alzheimer's disease. *Neurobiol. Aging* **17**, 733–743
44. DiPatre, P.L. and Gelman, B.B. (1997) Microglial cell activation in aging and Alzheimer disease: partial linkage with neurofibrillary tangle burden in the hippocampus. J. *Neuropathol. Exp. Neurol.* **56**, 143–149
45. El-Khoury, J., Hickman, S.E., Thomas, C.A., Loike, J.D., and Silverstein, S.C. (1998) Microglia, scavenger receptors, and the pathogenesis of Alzheimer's disease. *Neurobiol. Aging* **19**, S81–S84
46. Murphy, M.P. (1999) Nitric oxide and cell death. *Biochim. Biophys. Acta* **1411**, 401–414
47. Bonfoco, E., Krainc, D., Ankarcrona, M., Nicotera, P., and Lipton, S. A. (1995) Apoptosis and necrosis: two distinct events induced, respectively, by mild and intense insults with N-methyl-D-aspartate or nitric oxide/superoxide in cortical cell cultures. *Proc. Natl Acad. Sci. USA* **92**, 7162–7166
48. Chao, C.C., Hu, S., and Peterson, P.K. (1995) Glia, cytokines, and neurotoxicity. *Crit. Rev.Neurobiol.* **9**, 189–205
49. Monnier, V.M. and Cerami, A. (1984) Accelerated age-related browning of human collagen in diabetes mellitus. *Proc. Natl Acad. Sci. USA* **81**, 583–587
50. Bolaños, J.P. and Almeida, A. (2006) Modulation of astroglial energy metabolism by nitric oxide. *Antioxid. Redox Signal.* **8**, 955–965
51. Columbano, A. (1995) Cell death: current difficulties in discriminating apoptosis from necrosis in the context of pathological processes in vivo. *J. Cell. Biochem.* **58**, 181–190
52. O'Brien, M.C., Healy Jr, S.F., Raney, S.R., Hurst, J.M., Avner, B., Hanly, A., Mies, C., Freeman, J.W., Snow, C., Koester, S.K., and Bolton, W.E. (1997) Discrimination of late apoptotic/necrotic cells (Type III) by flow cytometry in solid tumors. *Cytometry* **28**, 81–89
53. Hooper, C. and Pocock, J.M. (2007) Chromogranin A activates diverse pathways mediating inducible nitric oxide expression and apoptosis in primary microglia. *Neurosci. Lett.* **413**, 227–232
54. Lincoln, T.M., Cornwell, T.L., Komalavilas, P., and Boerth, N. (1996) Cyclic GMP dependent protein kinase in nitric oxide signaling. *Methods Enzymol.* **269**, 149–166
55. Albina, J.E., Cui, S., Mateo, R.B., and Reichner, J.S. (1993) Nitric oxide-mediated apoptosisin murine peritoneal macrophages. *J. Immunol.* **150**, 5080–5085
56. McDaniel, M.L., Corbett, J.A., Kwon, G., and Hill, J.R. (1997) A role for nitric oxide and other inflammatory mediators in cytokine-induced pancreatic beta-cell dysfunction and destruction. *Adv. Exp. Med. Biol.* **426**, 313–319
57. Fehsel, K., Kroncke, K.D., Meyer, K.L., Huber, H., Wahn, V., and Kolb-Bachofen, V. (1995) Nitric oxide induces apoptosis in mouse thymocytes. *J. Immunol.* **155**, 2858–2865
58. Heneka, M.T., Loschmann, P.A., Gleichmann, M., Weller, M., Schulz, J.B., Wullner, U., and Klockgether, T. (1998) Induction of nitric oxide synthase and nitric oxide-mediated apoptosis in neuronal PC12 cells after stimulation with tumor necrosis factor-alpha/lipopolysaccharide. *J. Neurochem.* **71**, 88–94
59. Dimmeler, S., Haendeler, J., Nehls, M., and Zeiher, A.M. (1997) Suppression of apoptosis by nitric oxide via inhibition of interleukin-1-beta-converting enzyme (ICE)-like and cysteine protease protein (CPP)-32-like proteases. *J. Exp. Med.* **185**, 601–607
60. Kwon, Y.G., Min, J.K., Kim, K.M., Lee, D.J., Billiar, T.R., and Kim, Y.M. (2001) Sphingosine 1-phosphate protects human umbilical vein endothelial cells from serum-deprived apoptosis by nitric oxide production. *J. Biol. Chem.* **276**, 10627–10633
61. Sata, M., Kakoki, M., Nagata, D., Nishimatsu, H., Suzuki, E., Aoyagi, T., Sugiura, S., Kojima, H., Nagano, T., Kangawa, K., Matsuo, H., Omata, M., Nagai, R., and Hirata, Y. (2000) Adrenomedullin and nitric oxide inhibit human endothelial cell apoptosis via cyclic GMP-independent mechanism. *Hypertension* **36**, 83–88
62. Kim, Y.M., de Vera, M.E., Watkins, S.C., and Billiar, T.R. (1997) Nitric oxide protects cultured rat hepatocytes from tumor necrosis factor-alpha-induced apoptosis by inducing heat shock protein 70 expression. *J. Biol. Chem.* **272**, 1402–1411
63. Dash, P.R., Cartwright, J.E., Baker, P.N., Johnstone, A.P., and Whitley, G.S.J. (2003) Nitric oxide protects human extravillous trophoblast cells from apoptosis by cyclic GMP-dependent mechanism and independently of caspase 3 nitrosylation. *Exp. Cell Res.* **287**, 314–324
64. Taguchi, A., Blood, D.C., del Toro, G., Canet, A., Lee, D.C., Qu, W., Tanji, N., Lu, Y., Lalla, E., Fu, and Caifeng. (2000) Blockade of RAGE-amphoterin signalling suppresses tumour growth and metastases. *Nature* **405**, 354–360
65. Sladjana, D., Gasic-Milenkovic, J., Deuther-Conrad, W., and Munch, G. (2003) Signal transduction pathways in mouse microglia N-11 cells activated by advanced glycation endproducts (AGEs). *J. Neurochem.* **87**, 44–55